Inorganic Chemistry

Article

pubs.acs.org/IC

Fe as Hydrogen/Halogen Bond Acceptor in Square Pyramidal $Fe(CO)_5$

P. Aiswaryalakshmi, Devendra Mani, and E. Arunan*

Department of Inorganic and Physical Chemistry, Indian Institute of Science, Bangalore 560012, India

Supporting Information

ABSTRACT: Hydrogen bonded complexes formed between the square pyramidal $Fe(CO)_5$ with HX (X = F, Cl, Br), showing X-H···Fe interactions, have been investigated theoretically using density functional theory (DFT) including dispersion correction. Geometry, interaction energy, and large red shift of about 400 cm^{-1} in the HX stretching frequency confirm X-H···Fe hydrogen bond formation. In the $(CO)_5Fe$···HBr complex, following the significant red-shift, the HBr stretching mode is coupled with the carbonyl stretching modes. This clearly affects the correlation between frequency shift and binding energy, which is a hallmark of hydrogen bonds. Atoms in Molecule (AIM) theoretical analyses show the presence of a bond critical point between the iron and the hydrogen of HX and significant mutual penetration. These X-H···Fe hydrogen bonds follow most but not all of the eight criteria proposed by Koch and Popelier (*J. Phys. Chem.* **1995**, *99*, 9747) based on their investigations on C−H···O hydrogen bonds. Natural bond orbital (NBO) analysis indicates charge transfer from the organometallic system to the hydrogen bond donor. However, there is no correlation between the extent of charge transfer and interaction energy, contrary to what is proposed in the recent IUPAC recommendation (*Pure Appl. Chem.* **2011**, *83*, 1637). The "hydrogen bond radius" for iron has been determined to be 1.60 ± 0.02 Å, and not surprisingly it is between the covalent (1.27 Å) and van der Waals (2.0) radii of Fe. DFT and AIM theoretical studies reveal that Fe in square pyramidal $Fe(CO)_5$ can also form halogen bond with ClF and ClH as "halogen bond donor". Both these complexes show mutual penetration as well, though the Fe---Cl distance is closer to the sum of van der Waals radii of Fe and Cl in $(CO)_5Fe$···ClH, and it is about 1 Å less in $(CO)_5Fe$···ClF.

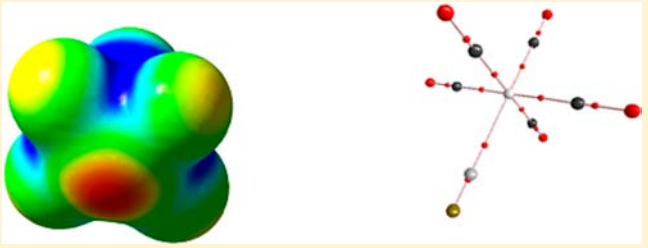

I. INTRODUCTION

Noncovalent interactions are primarily classified as van der Waals interaction and hydrogen bonding, and the boundary between the two has remained a topic of great interest. In the earlier days, the hydrogen bond was considered as the interaction between H atom bonded to a highly electronegative element X and another electro negative element Y which has a lone pair of electrons and is usually represented as X-H···Y. Conventional hydrogen bond acceptors are F, N, and O all having electronegativity significantly greater than hydrogen. Volumes of work have been done in this area.[1−4] Later developments in experimental and theoretical studies have revealed the presence of "nonconventional" hydrogen bonds. According to the new IUPAC definition,[5] the hydrogen bond is an attractive interaction between a hydrogen atom from a molecule or fragment X−H in which X is more electronegative than H, and an atom or a group of atoms in the same or a different molecule or fragment in which there is evidence of bond formation. While X was still restricted to being more electronegative than H, mainly to emphasize that H is partially positive, there was no restriction on Y. Lone pair electrons, π and sigma bonded electrons, an unpaired electron, hydrides, and even rare gas atoms can be hydrogen bond acceptors.[6−11] A technical report accompanying the IUPAC recommendation gives a summary of the various acceptors and donors for hydrogen bonds.[12]

One of the most active research areas in organic chemistry is the application of transition metals to organic synthesis. The transition metal can get involved in the three-center interactions. Some transition metals show a similar property as that of classical hydrogen bond acceptors, generating nonconventional hydrogen bonds. Metal interacting with hydrogen to form hydrogen bonding was first demonstrated by Trifan and Bacskai.[13] Interaction of transition metal centers with hydrogen atom has also been widely studied,[14−21] and the common metals which act as hydrogen bond acceptors are Au, Co, Ni, Pt, Ir, Ru, Os, and so on.

The ability of transition metals Co and Ni to form hydrogen bonded complexes were studied by Alkorta et al.[22] using $(CO)_4Co^-$ and $(CO)_4Ni$ as the hydrogen bond acceptors. The $(CO)_4Co^-$ forms strong hydrogen bond complex whereas $(CO)_4Ni$ is a very poor acceptor of hydrogen bonds. This difference was attributed to the presence of a charge in the $(CO)_4Co^-$. Interaction of M···HO bond in alpha- metallocenylcarbinols (M = Fe, Ru, Os) showed no evidence of Fe forming a hydrogen bond whereas Ru and Os did show such evidence.[23] The reason was ascribed to the basicity of Fe and steric factors. It occurred to us that the square pyramidal geometry of $Fe(CO)_5$ should have a dipole moment and should be able to form a hydrogen bond, in which dipole−dipole

Received: June 14, 2013
Published: July 8, 2013

dx.doi.org/10.1021/ic4015114 | *Inorg. Chem.* 2013, 52, 9153−9161

interactions do play a significant role. In the gas phase, square pyramidal geometry exists as a transition state during the Berry pseudorotation.[24] In fact, Rose-Petruck and co-workers[25,26] have observed $Fe(CO)_5\cdots C_6H_6$ complex in solution, with $Fe(CO)_5$ in square pyramidal geometry and one C−H group from C_6H_6 pointing toward Fe from the sixth coordination site. Somewhat surprisingly, another study by the same group[27] has shown that $Fe(CO)_5$ solvated in alcohols remains in trigonal bipyramidal geometry, forming a weak 1:1 complex with the solvent molecule. There was no evidence for bond formation between the two interacting moieties, though there was some charge transfer from the alcohol to the organometallic system. This is surprising as one would expect OH groups to be better in forming hydrogen bonds than the CH groups in benzene. Clearly, the stronger interaction between the alcohol molecules could have led to this observation. Studies on isolated complexes of $Fe(CO)_5$ would be useful. To the best of our knowledge, there has been no experimental or theoretical report of $Fe(CO)_5$ forming hydrogen bonds with typical donors, which is the main focus of this manuscript.

Iron pentacarbonyl is a yellow and oily liquid. It is pyrophoric in air and burns to Fe_2O_3 and decomposes by light to $Fe_2(CO)_9$ and CO. Trigonal bipyramid (D_{3h}) is the most stable geometry of iron pentacarbonyl, and it does not have a dipole moment. The square pyramidal geometry can have a dipole moment and interact with typical hydrogen bond donors, the energy separation being small. In this work, the interaction of $Fe(CO)_5$ with different hydrogen halides, HX (X = F, Cl, Br), are considered to explore whether $Fe(CO)_5$ can act as hydrogen bond acceptor. Ab initio density functional theory (DFT) calculations have been used to optimize the geometry and calculate the frequency shift in HX stretching. In addition, Atoms in Molecule (AIM) and natural bond orbital (NBO) analyses are carried out to characterize the interaction between $Fe(CO)_5$ and HX.

II. COMPUTATIONAL METHODS

Both square pyramidal and trigonal bipyramidal structures of iron pentacarbonyl were optimized with restricted symmetry using Gaussian03 and Gaussian09[28] at the B3LYP level of theory using large basis sets, 6-311++G**, Aug-cc-pVDZ and Aug-cc-pVTZ . As the B3LYP functional has been shown to perform poorly for non covalent interactions in particular for the dispersion contributions, several empirical corrections have been proposed in the literature.[29,30] We used the wB97XD functional with aug-ccpVTZ basis set and repeated all the calculations. We note that a recent study has shown this functional to recover the dispersion contributions significantly[30] and also that the specific example chosen in this study, square pyramidal $Fe(CO)_5$ has a significant dipole moment. For Fe, in all the calculations, only the 6-311++G** basis set was used. Frequency calculations were carried out for all the optimized geometries to affirm that they are true minima. Interaction energies were corrected for both zero point energies and basis set superposition error. The latter was calculated by the counterpoise method as implemented in Gaussian.[31] Bader's AIM theory[32] was used to study the electron density topology in the complexes to throw more light on the nature of interaction. The AIM2000[33] package was used to get the properties of all the critical points, including atoms. NBO analysis was done using NBO 6.0 software,[34] and the molecular electrostatic potential map calculations were done using Gaussian and GaussView.[35]

III. RESULTS AND DISCUSSION

III. A. Geometric Parameters, Frequency Shifts, and Interaction Energies. The molecular electrostatic potential map at the 0.0004 au iso-surface of the electron density of the square pyramidal $Fe(CO)_5$ calculated at the B3LYP/Aug-cc-pVTZ level is shown in Figure 1. The blue color represents the

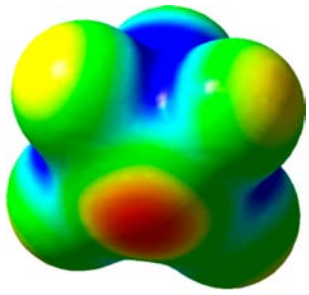

Figure 1. Molecular electrostatic potential map of $Fe(CO)_5$ at B3LYP/Aug-cc-pVTZ at 0.004 au iso-surface of electron density (red is negative and blue is positive).

region of positive potential, and the region of negative potential is given in red. The intermediate values of the electrostatic potential are represented by other colors, green, yellow, and so on. From the figure, the electrophilic region in the molecule can be located as the sixth coordination site of iron. Hence, any electron deficient species will tend to approach $Fe(CO)_5$ along this site. Moreover, the dipole moment of this structure at this level is 1.03 D, with Fe as the negative end. Not surprisingly, geometry optimizations and frequency calculations show that $Fe(CO)_5$ can form stable complexes with HX (X = F, Cl, Br), with the HX located at the sixth coordination site.

The optimized geometries of the complexes are shown in Figure 2, and the electrostatic potential maps of the complexes

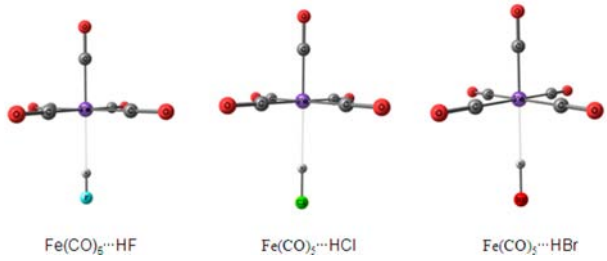

Figure 2. Optimized Geometries of $Fe(CO)_5\cdots HX$ Complexes (X = F, Cl, or Br) at B3LYP/Aug-cc-pVTZ.

of $Fe(CO)_5$ with HF, HCl, and HBr obtained at B3LYP/Aug-cc-pVTZ in Figure 3. The electrostatic potential maps show the results of charge transfer between $Fe(CO)_5$ and HX, which is discussed later along with the NBO analysis. All the geometrical parameters, energetics, and shift in IR stretching frequency of

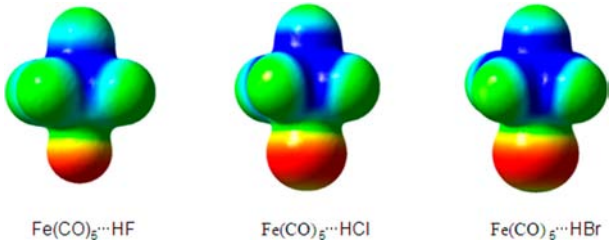

Figure 3. Molecular Electrostatic Potential Maps of $Fe(CO)_5\cdots HX$ Complexes (X = F, Cl, or Br) at B3LYP/Aug-cc-pVTZ at 0.004 au iso-surface of electron density (red is negative and blue is positive).

dx.doi.org/10.1021/ic4015114 | Inorg. Chem. 2013, 52, 9153−9161

Table 1. Optimized Fe−H Bond Distances (Å), ∠FeHX Bond Angles (deg), Change in H-X Distance (Δr Å), Shift in H-X Stretching Frequency ($\Delta\nu$ cm^{-1}), BSSE Corrected Interaction Energy (ΔE_{BSSE}), and Zero Point and BSSE Corrected Interaction Energy ($\Delta E_{ZPE(BSSE)}$), in kcal mol^{-1} for $Fe(CO)_5$···HX Complexes (X= F, Cl, or Br) at B3LYP/Aug-cc-pVTZ[a]

complex	R_{Fe-H}	∠XHFe	Δr	$\Delta\nu$	ΔE_{BSSE}	$\Delta E_{ZPE(BSSE)}$
$Fe(CO)_5$···HF	2.391 [2.353]	180.0 [180.0]	0.019 [0.020]	452.1 [463.0]	−3.8 [−7.2]	−2.3 [−5.8]
$Fe(CO)_5$···HCl	2.501 [2.443]	180.0 [180.0]	0.029 [0.029]	421.0 [388.6]	−3.2 [−5.0]	−2.2 [−3.9]
$Fe(CO)_5$···HBr	2.460 [2.422]	180.0 [180.0]	0.039 [0.036]	448.5[b] [429.0[b]]	−1.6 [−5.5]	−0.7 [−4.9]

[a]Values given in square brackets are calculated at the wB97XD/Aug-cc-pVTZ level. [b]In this complex, H−Br stretching couples with two of the C≡O stretching modes producing three linear combinations. See text.

HX at the B3LYP/aug-cc-pVTZ level as well as dispersion corrected wB97xD/Aug-cc-pVTZ level are summarized in Table 1. The Fe−H distances at B3LYP/Aug-cc-pVTZ level for $Fe(CO)_5$···HF/HCl/HBr are 2.39, 2.50, and 2.46 Å, respectively. The van der Waals radii of Fe and H are 2.0 Å and 1.2 Å, respectively,[36] and the covalent radii of iron and hydrogen are 1.27 Å and 0.3 Å. As expected for hydrogen bonded complexes, the Fe---H distances lie between the sum of covalent radii and the sum of van der Waals radii of Fe and H. In all the complexes the angle ∠XHFe is indeed linear, an important criterion for hydrogen bond formation unaffected by any secondary interaction. To include the effect of dispersion, calculations were repeated with the dispersion corrected functional wB97xD using the Aug-cc-pVTZ basis set. There were no drastic changes in the geometries except in the intermolecular $Fe(CO)_5$···HF/HCl/HBr distances. Not surprisingly, these became little shorter on inclusion of dispersion. The angle ∠XHFe was unaffected and remained linear, see Table 1.

The red-shift in the H-X frequency, $\Delta\nu$, upon complex formation is a crucial indicator of the strength of the hydrogen bond, and it is in general related to the increase in the H-X bond length, $\Delta R_{H\text{-}X}$. The H−F bond length in $Fe(CO)_5$···HF is 0.94 Å corresponding to ΔR_{H-F} of 0.02 Å at the B3LYP/Aug-cc-pVTZ level. This leads to a large red shift in HF stretching frequency of 452.1 cm^{-1}. This is significantly larger than the $\Delta\nu$ for even the H_2O···HF complex, calculated at the same level, of 329.0 cm^{-1}. Somewhat coincidentally ΔR_{H-F} is 0.02 Å for the H_2O···HF complex as well. A similar red shift has been observed in the complex of HF with Au.[16] Clearly, the transition metals, either alone or in an organometallic complex, can act as strong hydrogen bond acceptors.

The $\Delta R_{H\text{-}X}$ and $\Delta\nu$ computed at the same level for $Fe(CO)_5$···HCl/HBr are 0.03/0.04 Å and 421.0/448.5 cm^{-1}, respectively. Clearly, there is no correlation between $\Delta R_{H\text{-}X}$ and $\Delta\nu$, and it is not surprising as the donors are different. As the IUPAC report pointed out,[12] these correlations work better when the donors are kept the same while varying the acceptors. Still, the large red-shift calculated for the HBr complex was a surprise. The interaction energies do follow the expected trend. These are −3.8, −3.2, and −1.6 kcal mol^{-1} for $Fe(CO)_5$···HF, $Fe(CO)_5$···HCl, and $Fe(CO)_5$···HBr, respectively. Adding an empirical dispersion correction at the wB97xD/Aug-cc-pVTZ level led to an increase in the interaction energy for all the complexes. At this level, the $Fe(CO)_5$···HBr complex (ΔE_{BSSE} = −5.5 kcal/mol) is more stable than the $Fe(CO)_5$···HCl complex (ΔE_{BSSE} = −5.0 kcal/mol). With both the functionals, the red-shift calculated for HCl is smaller than that for HF, but it increases for HBr. A closer inspection reveals that in the $Fe(CO)_5$···HBr complex, there is significant mode mixing between HBr stretching and CO stretching modes. The H−Br stretching frequency, ν_{H-Br}, in the monomer at B3LYP/Aug-cc-pVTZ is 2624.6 cm^{-1}. In the complex the HBr stretching mode is coupled with two of carbonyl stretching modes resulting in three normal modes at 2065.5, 2088.3, and 2176.1 cm^{-1}. The $\Delta\nu$ was calculated using the mode with the largest value. Such mode mixing is common in halogen/lithium bonded complexes where it is difficult to establish a correlation between $\Delta\nu$ and interaction energy.[14] Clearly, one has to be careful while looking for such correlation even in hydrogen bonded complexes of HBr, because of its relatively low frequency vibration.

A comparison of the interaction energies of $Fe(CO)_5$···HX shows the highest binding energy for $Fe(CO)_5$···HF, and at the B3LYP level with all the basis sets the binding energy follows the pattern $Fe(CO)_5$···HF > $Fe(CO)_5$···HCl > $Fe(CO)_5$···HBr. There is a direct correlation with the dipole moment of HX. At the B3LYP/Aug-cc-pVTZ level, the dipole moments of H−F, H−Cl, and H−Br are 1.8 D, 1.1 D, and 0.8 D, and the dipole moment of $Fe(CO)_5$ is 1.03 D. Interaction energies (ΔE), BSSE corrected interaction energies (ΔE_{BSSE}), zero point energies (ΔE_{ZPE}), BSSE and ZPE corrected interaction energies ($\Delta E_{ZPE(BSSE)}$) of $Fe(CO)_5$···HX complexes at basis sets 6-311++G**, Aug-cc-pVDZ, and Aug-cc-pVTZ are given in the Supporting Information. They do follow the same trend, and these results are independent of any basis set effects. However, the trend changes when dispersion was taken into account by using the wB97xD functional. At the wB97xD/Aug-cc-pVTZ level, again the $Fe(CO)_5$···HF complex (ΔE_{BSSE} = −7.2 kcal/mol) is the most stable one. However, the $Fe(CO)_5$···HBr (ΔE_{BSSE} = −5.5 kcal/mol) becomes more stable than $Fe(CO)_5$···HCl (ΔE_{BSSE} = −5.0 kcal/mol) complex on dispersion correction, which seems reasonable.

A comparative study of the interaction energy of $Fe(CO)_5$ as H bond acceptor with standard acceptors has been done at the B3LYP/6-311++G** level. The various acceptors chosen from the literature[14] are lone pair (H_2O), π (C_2H_4), unpaired (CH_3) and σ (H_2) electrons, with HF as the hydrogen bond donor. The interaction energies are −10.1, −4.5, −3.3, and −0.9 kcal mol^{-1} for H_2O···HF, C_2H_4···HF, CH_3···HF, and H_2···HF complexes, respectively. The interaction energy of $Fe(CO)_5$···HF (−6.6 kcal mol^{-1}) falls between that of H_2O···HF and C_2H_4···HF. Complexes of $(CO)_4Co^-$ and $(CO)_4Ni$[22] with HF gave interaction energies −11.90 and −1.23 kcal mol^{-1} respectively. From the stabilization energies of all the complexes, it can be concluded that $Fe(CO)_5$ forms a strong hydrogen bonded complex. It acts as a strong hydrogen bond acceptor even being a neutral compound.

III. B. Atoms In Molecules Analysis. Detailed AIM analyses have been carried out on all the three $Fe(CO)_5$···HX complexes to study the nature of the bond formed between iron and hydrogen using AIM 2000 software. According to Bader the presence of a (3,−1) critical point or bond critical point (BCP), along the bond path connecting the two

dx.doi.org/10.1021/ic4015114 | Inorg. Chem. 2013, 52, 9153−9161

interacting atoms is a necessary and sufficient condition to ascertain that the two atoms are bonded. Koch and Popelier[37] have proposed seven more criteria which should be satisfied for a bond to be called hydrogen bond. These criteria were suggested following investigations on various C−H···O contacts. Among these eight criteria, they pointed out that the mutual penetration of hydrogen and acceptor atoms is a necessary and sufficient condition. The $(CO)_5Fe\cdots HX$ complexes follow the necessary and sufficient conditions put forward by both Bader and Koch and Popelier, but they do not follow some of the criteria given by Koch and Popelier. All the results obtained at the B3LYP and wB97xD/Aug-cc-pVTZ levels are given in Tables 2, 3, and 4 and are discussed in detail

Table 2. Electron Density, ρ (a.u) and Laplacian of Electron Density, L (a.u) at H-Bond Critical Point of $Fe(CO)_5\cdots HX$ Complexes (X = F, Cl, or Br) at B3LYP/Aug-cc-pVTZ[a]

	$Fe(CO)_5\cdots HF$	$Fe(CO)_5\cdots HCl$	$Fe(CO)_5\cdots HBr$
ρ(bcp)	0.0199 [0.0214]	0.0177 [0.0193]	0.0194 [0.0207]
L	−0.0060 [-0.0062]	−0.0059 [-0.0064]	−0.0060 [-0.0065]

[a]Values given in square brackets are calculated at the wB97XD/Aug-cc-pVTZ level.

Table 3. Penetration: Bonded (r^b) and Non-bonded (r°) Radii (in Angstroms) of Acceptor (Fe) and Donor (H) Atoms and Penetration, Δr, Defined as the Sum of the Differences in Bonded and Non-bonded Radii of Fe and H at B3LYP/Aug-cc-pVTZ

complex	r°_{Fe}	r^b_{Fe}	$r^\circ_{Fe} - r^b_{Fe}$	r°_H	r^b_H	$r^\circ_H - r^b_H$	Δr
$Fe(CO)_5\cdots HF$	2.43	1.59	0.84	1.17	0.83	0.34	1.18
$Fe(CO)_5\cdots HCl$	2.43	1.62	0.81	1.27	0.90	0.37	1.18
$Fe(CO)_5\cdots HBr$	2.43	1.59	0.84	1.31	0.90	0.42	1.25

Table 4. Change in the Atomic Population, Atomic Energies, Atomic First Moment and Atomic Volume (a.u) of $Fe(CO)_5\cdots HX$ Complexes (X = F, Cl or Br) at B3LYP/Aug-cc-pVTZ[a]

	ΔN	ΔE	ΔM	ΔV
$Fe(CO)_5\cdots HF$	0.0579	−0.0037	0.0258	−1.2155
$Fe(CO)_5\cdots HCl$	0.0226	0.0229	0.0151	−1.3373
$Fe(CO)_5\cdots HBr$	−0.0007	0.0342	0.0187	−3.5885

[a]Δ = complex − monomer.

next. Complete results obtained at the B3LYP level with basis sets 6-311++G**, Aug-cc-pVDZ, and Aug-cc-TZ are given in the Supporting Information, and they follow similar trends.

Criteria for Hydrogen Bonding. *(1). Topology.* In all the complexes there is a bond critical point between the hydrogen atom and the acceptor atom, Fe, which are linked by a linear bond path. The structure of the complexes with bond critical points and bond baths are shown in Figure. 4.

(2). Charge Density at the Bond Critical Point (ρ). Koch and Popelier have proposed a range for the charge density at the BCP for a bond to be classified as hydrogen bond. The values of ρ at the bond critical point connecting Fe and H are 0.0199, 0.0177, and 0.0194 au at the B3LYP/Aug-cc-pVTZ level and 0.0214, 0.0193, and 0.0207 au at the wB97xD/Aug-cc-pVTZ level for complexes of $Fe(CO)_5$ with HF, HCl, and HBr, respectively. These values are within the range suggested by Koch and Popelier and are toward the upper limit.

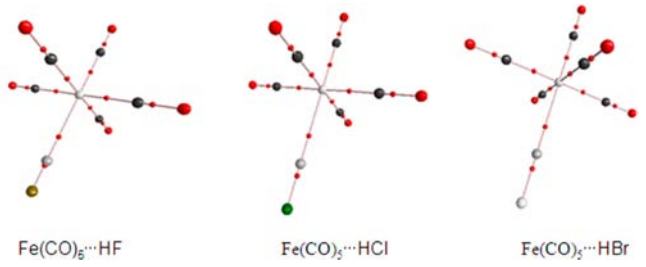

Figure 4. Structures of $Fe(CO)_5\cdots HX$ Complexes (X = F, Cl, or Br) with Bond Critical Points at the B3LYP/Aug-cc-pVTZ level.

(3). Laplacian of the Charge Density at the Bond Critical Point (L). The third criterion is about the Laplacian of the charge density at the hydrogen bond critical point. The L values for the complexes $Fe(CO)_5\cdots HF$, $Fe(CO)_5\cdots HCl$, and $Fe(CO)_5\cdots HBr$ at the B3LYP/Aug-cc-pVTZ level are −0.0060, −0.0059, and −0.0060 au and at the wB97xD/Aug-cc-pVTZ level, these are −0.0062, −0.0064, and −0.0065, respectively. All these values are within the range suggested by Koch and Popelier. The negative sign of L implies a closed-shell interaction, expected for typical hydrogen bonds.

(4). Mutual Penetration of Hydrogen and Acceptor Atom. The distance from the nucleus to the electron density contour 0.001 a.u along the bond path is defined as the nonbonded radius, r°, and the distance from the nucleus to the bond critical point is defined as the bonded radius, r^b. The difference between the bonded and nonbonded radii gives the extent of penetration. If there is penetration of electron cloud of hydrogen and acceptor atoms, Δr will be positive and it indicates bond formation. The values of r°, r^b, and Δr for $Fe(CO)_5\cdots HX$ (X = F, Cl, Br) at the B3LYP/Aug-cc-pVTZ level are given in Table 3. All the complexes show significant mutual penetration of the electron cloud, and the values for $Fe(CO)_5\cdots HF$, $Fe(CO)_5\cdots HCl$, and $Fe(CO)_5\cdots HBr$ are 1.18, 1.18, and 1.25 Å, respectively.

(5). Loss of Charge of Hydrogen Atom (ΔN). There should be a decrease in charge population of the hydrogen atom upon complex formation according to the fifth criteria proposed by Koch and Popelier. The $Fe(CO)_5\cdots HBr$ complex follows this criterion, and the decrease in population is 0.0007 au. However, there is an increase in the population upon complex formation in $Fe(CO)_5\cdots HF$ and $Fe(CO)_5\cdots HCl$, and these are significantly higher, 0.0579 and 0.0226 a.u, respectively, at the B3LYP/Aug-cc-pVTZ level, see Table 4.

(6). Change in Atomic Energy (ΔE). The sixth criterion deals with destabilization of hydrogen atom. This is due to the decrease in the total atomic energy of the hydrogen atom in the hydrogen bonded complex compared with that in the monomer. The hydrogen atom shows a loss in the total atomic energy in the $Fe(CO)_5\cdots HCl$ and $Fe(CO)_5\cdots HBr$ complexes. The magnitude of the destabilizations of the hydrogen atoms are 0.0229 and 0.0342 au, respectively. However, it shows an increase in stability in the $Fe(CO)_5\cdots HF$ complex, that is, the hydrogen of HF on interaction with $Fe(CO)_5$ gets more stabilized. The magnitude of stabilization of H on complexation is 0.0037 a.u. at the B3LYP/Aug-cc-pVTZ level.

(7). Change in Atomic First Moment (ΔM). The dipolar polarization of the hydrogen atom is expected to decrease on complex formation because of the loss of nonbonding density of hydrogen. Nevertheless hydrogen in the complexes, $Fe(CO)_5\cdots HF$, $Fe(CO)_5\cdots HCl$, $Fe(CO)_5\cdots HBr$, shows an

dx.doi.org/10.1021/ic4015114 | Inorg. Chem. 2013, 52, 9153−9161

Table 5. Natural Atomic Charge on Each Atom and the Charged Transferred (ΔQ,e) at B3LYP/Aug-cc-pVTZ[a]

complex	q(Fe)	q(C)eq	q(C)ax	q(O)eq	q(O)ax	ΔQ
$Fe(CO)_5$	−0.468 [−0.510]	0.551 [0.565]	0.521 [0.526]	−0.451 [−0.455]	−0.454 [−0.459]	
$Fe(CO)_5$···HF	−0.553 [−0.591]	0.564 [0.577]	0.531 [0.532]	−0.438 [−0.440]	−0.444 [−0.446]	0.038 [0.043]
$Fe(CO)_5$···HCl	−0.534 [−0.566]	0.564 [0.578]	0.537 [0.539]	−0.439 [−0.444]	−0.447 [−0.450]	0.056 [0.059]
$Fe(CO)_5$···HBr	−0.532 [−0.575]	0.569 [0.580]	0.546 [0.545]	−0.440 [−0.441]	−0.449 [−0.448]	0.081 [0.078]

[a]Values given in square brackets are calculated at wB97XD/Aug-cc-pVTZ.

increase in the dipolar polarization on formation of hydrogen bond. The changes in the atomic first moments for the hydrogen bond donors HF, HCl, and HBr at the B3LYP/Aug-cc-pVTZ level are given in Table 4.

(8). Change in Atomic Volume (ΔV). The eighth criterion is a decrease in the volume of the hydrogen atom upon complex formation. The hydrogen atoms participating in the hydrogen bond formation in all the three complexes follow this criterion. The volume of the hydrogen atom in the complexes is less than that in the monomer.

The Koch and Popelier criteria, evolved from analyzing C−H···O contacts, have become very popular. However, as the results presented above show, these may not be applicable to all the hydrogen bonded complexes. On the basis of our experience, we propose that the presence of a bond critical point and positive mutual penetration can be used as evidence based on AIM theory for a hydrogen bond. As mentioned earlier, these results do not change with basis sets.

III. C. NBO Analysis. To estimate the charge transfer between the hydrogen bond donor and acceptor, NBO analysis of $Fe(CO)_5$···HX (X = F, Cl, Br) at the B3LYP level with basis sets 6-311++G**, Aug-cc-pVDZ, and Aug-cc-pVTZ as well as at the wB97xD/Aug-cc-pVTZ level has been carried out. Charges on each of the atoms of $Fe(CO)_5$ and the difference on complex formation, that is, charge transferred, ΔQ at B3LYP/Aug-cc-pVTZ and wB97xD/Aug-cc-pVTZ level, are listed in Table 5. The values of ΔQ show that the charge is transferred from the organometallic system to the hydrogen bond donor. These values are 0.038, 0.056, and 0.081 e for $Fe(CO)_5$···HF/HCl/HBr, respectively, at the B3LYP/Aug-cc-pVTZ level. At the wB97xD/Aug-cc-pVTZ level, including dispersion, these values are slightly different, but the order remains the same. The net charge transfers at this level are 0.043, 0.059, and 0.078 e, respectively. At the same level of calculations, the FH···$Fe(CO)_5$ complex is much stronger than the other two, which both have very similar binding energies. Clearly, there is no direct correlation between the extent of electron transfer and binding energy for these complexes. This is contrary to the recent IUPAC recommendation,[5] which says the interaction energy is directly related to the charge transferred. However, the accompanying IUPAC technical report[12] does point out the complexities involved in generalizing hydrogen bond properties. In these complexes, the interaction energy is directly related to the dipole moment of the hydrogen bond donor and of course the IUPAC recommendation does say this. Clearly, in these complexes, the stabilization is primarily due to electrostatic forces. Charge transfer is significant too but does not appear to have any direct relation with the stability. There are indeed hydrogen bonded complexes in which charge transfer is the primary force. For example, the radical complex, XH···CF_3 (X = F, Cl, Br) are charge transfer assisted, with the interaction energy decreasing with increasing dipole moment but increasing with increasing charge transfer: FH···CF_3 < ClH···CF_3 < BrH···CF_3.[38]

NBO second order perturbation energies for these complexes are given in Table 6 at both the B3LYP/Aug-cc-pVTZ and the wB97xD/Aug-cc-pVTZ levels which show that charge is transferred from the nonbonding orbital of Fe to the antibonding orbital ($\sigma^*_{H\text{-}X}$) of HX. The analysis shows small charge transfer from the Fe−C bonding orbital to the $\sigma^*_{H\text{-}X}$ as well, more significant for the equatorial Fe−C bonds, which is expected due the complex nature of hydrogen bond acceptor moiety.

Table 6. Second Order Perturbation Energies $E^{(2)}$(donor → acceptor) in kcal mol^{-1}, Involving Non-Bonding Orbital of Donor and Antibonding Orbital of Acceptor

	$E^{(2)}(nB \rightarrow \sigma^*_{H\text{-}X})$ in kcal mol^{-1}	
complex	at B3LYP/Aug-cc-pVTZ	at wB97XD/Aug-cc-pVTZ
$Fe(CO)_5$···HF	3.51	5.08
$Fe(CO)_5$···HCl	3.03	5.06
$Fe(CO)_5$···HBr	3.45	5.81

III. D. $Fe(CO)_5$ as Chlorine Bond Acceptor. Halogen bonds are similar to hydrogen bonds except in this case halogen atom participates in bonding instead of hydrogen. Halogen bonds have recently gained immense popularity,[39,40] and among halogen bonds, chlorine bond is the most popular.[41] Since Fe is a good acceptor of hydrogen bonds, comparable to the conventional hydrogen bond acceptors, we wanted to verify whether Fe can take part in chlorine bonding. ClF and HCl were chosen as the chlorine bond donors, and their interactions with $Fe(CO)_5$ were examined. Geometry optimizations were done with the B3LYP functional and also the dispersion corrected wB97xD functional. Frequency analysis showed that geometries optimized with both 6-311G** and 6-311++G** basis sets were true minima for $Fe(CO)_5$···ClF complex whereas for $Fe(CO)_5$···ClH minima could be obtained only with 6-311G** basis set. In the optimized geometries chlorine interacts with Fe in the same way as hydrogen does in the analogous HX complexes, that is, along the sixth coordination site.

$Fe(CO)_5$···ClF. R_{Fe-Cl} distances in $Fe(CO)_5$···ClF are 2.60 Å and 2.53 Å at 6-311G** and 6-311++G**, respectively, and the corresponding change in Cl−F bond lengths are very large, 0.21 and 0.27 Å. The van der Waals radius of Fe is 2.0 Å and that for Cl is 1.7 Å. The bond angles ∠FClFe calculated at both basis sets are 180.0°. Because of mode mixing, none of the normal mode vibrations in the complex can be assigned to pure Cl−F stretching. The complex has very high interaction energy and with the B3LYP functional, the BSSE corrected interaction energies are −13.57 kcal mol^{-1} and −18.88 kcal mol^{-1} 6-311G** and 6-311++G** basis sets, respectively. As found for the hydrogen bonded complexes, adding dispersion at the wB97xD/6-311++G** level leads to a small change, and the binding energy is reduced to −15.88 kcal mol^{-1}.

dx.doi.org/10.1021/ic4015114 | Inorg. Chem. 2013, 52, 9153−9161

Table 7. Penetration: Bonded (r^b) and Non-bonded ($r°$) Radii (in Angstroms) of Acceptor (Fe) and Donor (Cl) Atoms and Penetration, Δr, Defined as the Sum of the Differences in Bonded and Non-bonded Radii of Fe and Cl in $Fe(CO)_5$···ClF and in $Fe(CO)_5$···ClH at the B3LYP Level

complex	basis set	$r°_{Fe}$	r^b_{Fe}	$r°_{Fe} - r^b_{Fe}$	$r°_{Cl}$	r^b_{Cl}	$r°_{Cl} - r^b_{Cl}$	Δr
$Fe(CO)_5$···ClF	6-311G**	2.24	1.28	0.96	1.81	1.32	0.49	1.45
	6-311++G**	2.39	1.22	1.17	1.82	1.31	0.51	1.68
$Fe(CO)_5$···ClH	6-311G**	2.24	1.93	0.31	1.94	1.79	0.15	0.46

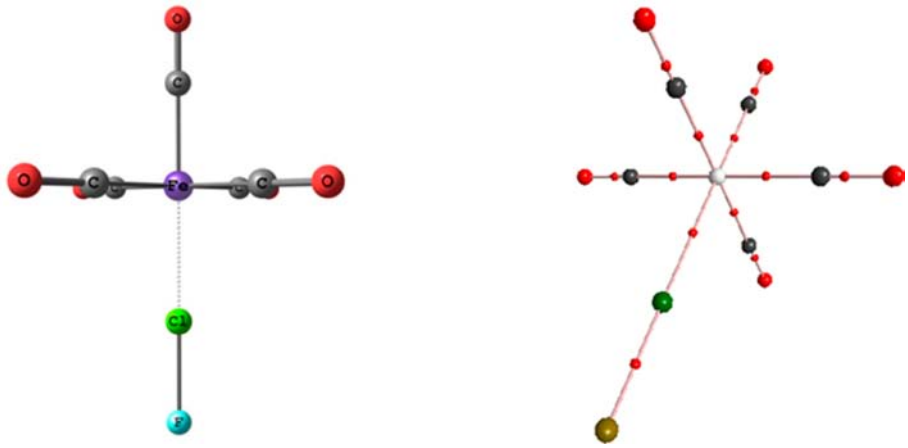

Figure 5. Optimized Geometry and AIM Structure with Bond Critical Points of $Fe(CO)_5$···ClF at B3LYP/6-311++G**.

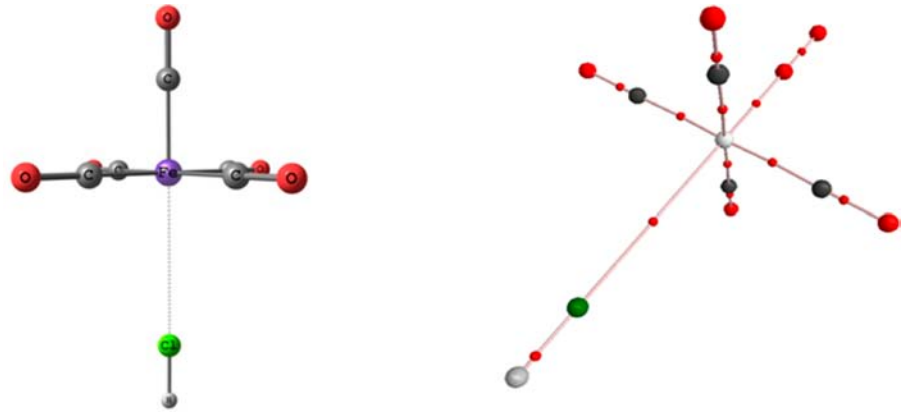

Figure 6. Optimized Geometry and AIM Structure with Bond Critical Points of $Fe(CO)_5$···ClH at B3LYP/6-311G**.

The high stabilization energies for this complex can be explained using AIM analysis, which indeed shows a bond critical point between Fe and Cl. The electron density calculated at the bond critical point (ρ) between Fe and Cl is 0.0427 a.u and 0.0497 a.u with the B3LYP functional and 6-311G** and at 6-311++G** basis sets, respectively. These values are more than double of the calculated values for the hydrogen bonded complexes (see Tables 2, 3, and 4). The high electron density indicates more electron accumulation between Fe and Cl. This is reflected in the mutual penetration of Fe and Cl atoms as well. The penetrations of Fe at 6-311G** and 6-311++G** are 0.96 and 1.17 Å, respectively, and those of Cl are 0.49 and 0.51 Å, respectively. Thus, the mutual penetrations at both the basis sets are 1.45 and 1.68 Å, respectively. The bonded radius of Fe is 1.2778 Å which is very close to the covalent radius of Fe, 1.27 Å. The bonded radius of chlorine in ClF, 1.32 Å, is within the range of the chlorine bond radius for ClF (1.28 ± 0.11 Å).[42] Hence in $Fe(CO)_5$···ClF, the Fe···Cl interaction is more covalent than the corresponding hydrogen bonded complexes. The bonded and nonbonded radii of Fe and Cl are given in Table. 7. The optimized geometries and the AIM structure with bond critical point and bond path are shown in Figure 5. While all these results point toward a more covalent nature in the $(CO)_5$Fe···ClF interaction, the Laplacian (L) values calculated are −0.0139 a.u. and −0.0148 a.u. at the two basis sets used. This is typical of a closed shell interaction rather than shared shell interaction.

$Fe(CO)_5$···ClH. At B3LYP/6-311G** level, the Fe−Cl distance (R_{Fe-Cl}) in $Fe(CO)_5$···ClH is 3.72 Å and the ∠HClFe bond angle is linear. Clearly the distance is almost exactly equal to the sum of van der Waals radii of Fe and Cl. Is this enough to conclude that the interaction is just van der Waals? The change in the Cl−H bond length is 0.003 Å, an order of magnitude smaller than found for ClF. However, the shift in the Cl−H stretching frequency on complexation is 40.9 cm^{-1}, which is quite significant for a HCl complex. $Fe(CO)_5$···ClH has a very low stabilization energy, −0.75 kcal mol^{-1}, compared to the $Fe(CO)_5$···ClF complex. The

dx.doi.org/10.1021/ic4015114 | Inorg. Chem. 2013, 52, 9153−9161

electron density at the bond critical point (ρ) between Fe and Cl is 0.0048 a.u and its Laplacian (L) is −0.0036 a.u, both within the range suggested by Koch and Popelier for C−H···O hydrogen bonds. The electron density at the bond critical point is 1 order of magnitude less than that for $Fe(CO)_5$···ClF complex. This explains the huge difference in the stabilization energy. However, Fe and Cl do show mutual penetration of a significant 0.46 Å, despite the distance between Fe and Cl being close to the sum of their van der Waals radii. This is because the nonbonded radii from AIM calculations for Fe and Cl are 2.24 and 1.94 Å, respectively. Clearly, blind use of van der Waals radii to conclude about intermolecular interactions is not advisable. The nonbonded and bonded radii of Fe and Cl are given in Table.7. The optimized geometries and the AIM structure with bond critical point and bond path are shown in Figure. 6.

NBO analysis has been carried out to assay the influence of charge transfer on the stability of both theses complex. From the NBO analysis of $Fe(CO)_5$···ClF and $Fe(CO)_5$···ClH complexes at the B3LYP/6-311G** level, the amount of charge transferred from $Fe(CO)_5$, ΔQ, is positive. This means, charge is transferred from the organometallic system to the chlorine bond donor. The amount of charge transferred from $Fe(CO)_5$ is 0.518e and 0.024e for $Fe(CO)_5$···ClF and $Fe(CO)_5$···ClH, respectively. The ΔQ for $Fe(CO)_5$···ClH is comparable to that of $Fe(CO)_5$···HX complexes, though slightly smaller. $Fe(CO)_5$···ClF shows a huge charge transfer from $Fe(CO)_5$ to the chlorine bond donor, which is consistent with the AIM analysis discussed above.

The high ΔE, ΔQ, and ρ at the bond critical point between Fe and Cl in the $Fe(CO)_5$···ClF complex can be explained on the basis of the σ-hole concept.[39] The molecular electrostatic potential maps of ClF and ClH are shown in Figure. 7. The

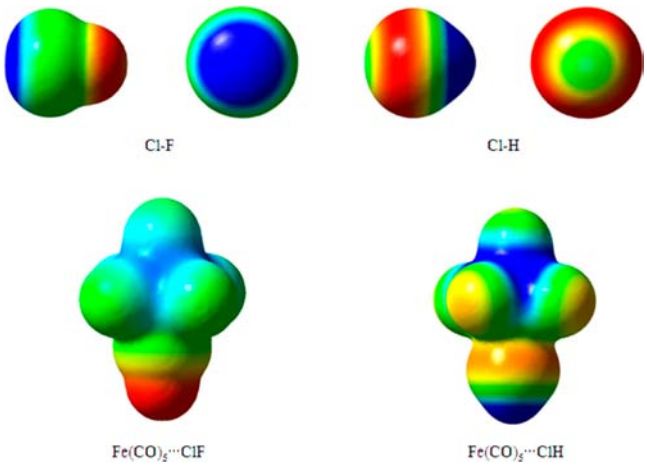

Figure 7. Molecular Electrostatic Potential Maps of Cl−F, Cl−H, $Fe(CO)_5$···ClF, and $Fe(CO)_5$···ClH complexes at B3LYP/6-311G** at 0.004 au iso-surface of electron density (red is negative and blue is positive).

positive potential around chlorine in ClF is quite significant and much larger than that found in ClH. Clearly the electronegativity differences between the three atoms contribute to this. However, even in ClH, there is a positive potential around Cl, though Cl is more electronegative than H. Because of the presence of high positive potential on chlorine in Cl−F, it interacts strongly with $Fe(CO)_5$. The higher charge transfer from $Fe(CO)_5$ to Cl−F is also obvious from the electrostatic map, see Figure 7. In $Fe(CO)_5$···ClF, there is a huge depletion of negative potential at the oxygen atoms after complex formation. Whereas, even after complexation there is high negative potential around the oxygen atoms in $Fe(CO)_5$···ClH, since the charge transferred from $Fe(CO)_5$ to Cl−H is less.

III. E. Hydrogen Bond Radius of Iron. The bonded radius of elements varies with the interacting partner as is clear from Table 3 and Table 7. Hence it will not be appropriate to use the van der Waals radii for all interactions. In the books on hydrogen bonding by Jeffrey and Saengar[43] and Desiraju and Steiner,[2] the authors have pointed out the inadequacy of van der Waals radii for identifying hydrogen bonding. The recent IUPAC recommendation has discouraged the use of van der Waals radii to conclude/rule out the presence of a hydrogen bond as well.[5] Klein[44] and Mandal and Arunan[45] have independently pointed out that more specific radii for various atoms can be used for hydrogen bonding. Later Raghavendra et al.[46] have reported the hydrogen bond radii of various acceptors and donors using ab initio and AIM methods. In a hydrogen bonded complex X-H···Y, the hydrogen bond radius for the donor is simply the distance between the H and BCP and that of the acceptor is the distance between the BCP and Y. The data presented for $Fe(CO)_5$···HX (X = F, Cl, Br) complexes present us with an opportunity not only for verifying the hydrogen bond radii for HX but also to determine the hydrogen bond radii for Fe. At the B3LYP/Aug-cc-pVTZ level, the distances between BCP and Fe atom are 1.5899, 1.6200, and 1.5851 Å for $Fe(CO)_5$···HF, $Fe(CO)_5$···HCl and $Fe(CO)_5$···HBr, respectively. From these values, the hydrogen bond radius of Fe is determined as 1.60 (±0.02) Å. This may be compared with the van der Waals radius of Fe, 2.0 Å, and covalent radius of Fe, 1.27 Å. Moreover, the hydrogen bond radii for HF, HCl, and HBr are 0.83, 0.90, and 0.90 Å, respectively. These are closer to the hydrogen bond radii recommended for medium hydrogen bonds, 0.89 Å.

IV. CONCLUSIONS

Interaction of hydrogen halides, HX (X = F, Cl, Br), with the square pyramidal geometry of iron pentacarbonyl have been investigated. The hydrogen of HX interacts with Fe through the sixth co-ordination site. These complexes show most of the characteristics typical of hydrogen bond interaction. The large red shift in the H-X stretching frequency on complex formation supports this. In $Fe(CO)_5$···HBr, there is mode mixing between the H−Br and the C═O stretching frequencies. AIM analysis of the complexes shows the presence of a bond critical point between the iron and the hydrogen of HX. Though, these complexes do not follow all the criteria proposed by Koch and Popelier for hydrogen bonding, they do follow the necessary and sufficient conditions. There is significant mutual penetration of the Fe and H atoms involved in hydrogen bonding. NBO analysis confirms charge transfer from the organometallic system to the hydrogen bond donor, though there is no correlation between the amount of charge transferred and interaction energies. The interaction energies are proportional to the dipole moment of the hydrogen bond donor. Using ClF and ClH as chlorine bond donors, the potentiality of Fe to act as chlorine bond acceptor is examined. Optimized geometries and the AIM analysis do confirm that Fe can act as chlorine bond acceptor as well. The huge difference in the stabilization energy and in the amount of charge transferred between $Fe(CO)_5$···ClF and $Fe(CO)_5$···ClH can be understood from the σ-hole concept. Both complexes show significant mutual

dx.doi.org/10.1021/ic4015114 | Inorg. Chem. 2013, 52, 9153−9161

penetration, though the distance between Fe and Cl is very close to the sum of their van der Waals radii in $Fe(CO)_5\cdots ClH$ complex. Our studies conclusively show that $Fe(CO)_5$ can act as a strong hydrogen and chlorine bond acceptor, even being a neutral compound. This stabilizes the square pyramidal geometry of iron pentacarbonyl, which is considered a saddle point. The hydrogen bond radius of Fe has been determined as 1.60(±0.02) Å.

■ ASSOCIATED CONTENT

Supporting Information

Interaction energies (ΔE), BSSE corrected interaction energies (ΔE_{BSSE}), zero point energies (ΔE_{ZPE}), BSSE corrected zero point energies ($\Delta E_{ZPE(BSSE)}$), and complete structural information for all the minima found by calculations and all AIM parameters calculated with various basis sets are given in nine tables. This material is available free of charge via the Internet at http://pubs.acs.org.

■ AUTHOR INFORMATION

Corresponding Author

*E-mail: arunan@ipc.iisc.ernet.in. Phone: +91-80-2293-2828. Fax: +91-80-2360-0282.

Notes

The authors declare no competing financial interest.

■ ACKNOWLEDGMENTS

We acknowledge funds from the Department of Science and Technology, Indo-French Centre for Promotion of Advanced Research, and Indian Institute of Science. We thank the Supercomputer Education and Research Centre for use of their computing facility. D.M. thanks CSIR-India for a research fellowship. We thank Prof. G. Naresh Patwari who brought reference 27 to our notice and which led us to this work. We thank Prof. Frank Weinhold and Prof. Ibon Alkorta for useful discussions about NBO calculations.

■ REFERENCES

(1) Scheiner, S. *Hydrogen Bonding A Theoretical Perspective*; Oxford University Press: Oxford, U.K., 1997.

(2) Desiraju, G. R.; Steiner, T. *The Weak Hydrogen Bond: In Structural Chemistry and Biology*; Oxford University Press: Oxford, U.K., 1999.

(3) Pauling, L. *The Nature of the Chemical Bond*; Cornell University Press: Ithaca, NY, 1960.

(4) Jeffrey, G. A. *Introduction to Hydrogen Bonding*; Oxford University Press: Oxford, U.K., 1997.

(5) Arunan, E.; Desiraju, G. R.; Klein, R. A.; Sadlej, J.; Scheiner, S.; Alkorta, I.; Clary, D. C.; Crabtree, R. H.; Dannenberg, J. J.; Hobza, P.; Kjaergaard, H. G.; Legon, A. C.; Mennucci, B.; Nesbitt, D. J. *Pure. Appl. Chem.* **2011**, *83*, 1637−1641.

(6) Alkorta, I.; Rozas, I.; Elguero, J. *Chem. Soc. Rev.* **1998**, *27*, 163−170.

(7) Crabtree, R. H. *J. Organomet. Chem.* **1998**, *577*, 111−115.

(8) Szymczak, J. J.; Grabowski, S. J.; Roszak, S.; Leszczynski, J. *Chem. Phys. Lett.* **2004**, *393*, 81−86.

(9) Grabowski, S. J.; Sokalski, W. A.; Leszczynski, J. *Chem. Phys. Lett.* **2006**, *432*, 33−39.

(10) Raghavendra, B.; Arunan, E. *J. Phys. Chem. A.* **2007**, *111*, 9699−9706.

(11) Raghavendra, B.; Arunan, E. *Chem. Phys. Lett.* **2008**, *467*, 37−40.

(12) Arunan, E.; Desiraju, G. R.; Klein, R. A.; Sadlej, J.; Scheiner, S.; Alkorta, I.; Clary, D. C.; Crabtree, R. H.; Dannenberg, J. J.; Hobza, P.; Kjaergaard, H. G.; Legon, A. C.; Mennucci, B.; Nesbitt, D. J. *Pure. Appl. Chem.* **2011**, *83*, 1619−1636.

(13) Trifan, D. S.; Bacskai, R. *J. Am. Chem. Soc.* **1960**, *82*, 5010−5011.

(14) Kryachko, E. S.; Karpfen, A.; Remacle, F. *J. Phys. Chem. A* **2005**, *109*, 7309−7318.

(15) Brammer, L.; Zhao, D.; Ladipo, F. T.; Braddock-Wilking, J. *Acta Crystallogr.* **1995**, *B51*, 632−640.

(16) Braga, D.; Grepioni, F.; Tedesco, E.; Biradha, K.; Desiraju, G. R. *Organometallics* **1997**, *16*, 1846−1856.

(17) Brammer, L. *Dalton Trans.* **2003**, 3145−3157.

(18) Martin, A. *J. Chem. Educ.* **1999**, *76*, 578−583.

(19) Grabowski, S. J.; Leszczynski, J. *Hydrogen Bonding: New Insights*; Springer: Dordrecht, The Netherlands, 2006.

(20) Kryachko, E. S. *J. Mol. Struct.* **2008**, *880*, 23−30.

(21) Natale, D.; Mareque-Rivas, J. C. *Chem. Commun.* **2008**, 425−437.

(22) Alkorta, I.; Rozas, I.; Elguero, J. *J. Mol. Struct.: THEOCHEM* **2001**, *537*, 139−150.

(23) Orlova, G.; Scheiner, S. *Organometallics* **1998**, *17*, 4362−4367.

(24) Berry, R. S. *J. Chem. Phys.* **1960**, *32*, 933−938.

(25) Jiang, Y.; Lee, T.; Rose-Petruck, C. G. *J. Phys. Chem. A* **2003**, *107*, 7524−7538.

(26) Lee, T.; Benesch, F.; Jiang, Y.; Rose-Petruck, C. G. *Chem. Phys.* **2004**, *299*, 233−245.

(27) Lessing, J.; Li, X.; Lee, T.; Rose-Petruck, C. G. *J. Phys. Chem. A* **2008**, *112*, 2282−2292.

(28) (a) Frisch, M. J.; Trucks, G. W.; Schlegel, H. B.; Scuseria, G. E.; Robb, M. A.; Cheeseman, J. R.; Montgomery, Jr., J. A.; Vreven, T.; Kudin, K. N.; Burant, J. C.; Millam, J. M.; Iyengar, S. S.; Tomasi, J.; Barone, V.; Mennucci, B.; Cossi, M.; Scalmani, G.; Rega, N.; Petersson, G. A.; Nakatsuji, H.; Hada, M.; Ehara, M.; Toyota, K.; Fukuda, R.; Hasegawa, J.; Ishida, M.; Nakajima, T.; Honda, Y.; Kitao, O.; Nakai, H.; Klene, M.; Li, X.; Knox, J. E.; Hratchian, H. P.; Cross, J. B.; Bakken, V.; Adamo, C.; Jaramillo, J.; Gomperts, R.; Stratmann, R. E.; Yazyev, O.; Austin, A. J.; Cammi, R.; Pomelli, C.; Ochterski, J. W.; Ayala, P. Y.; Morokuma, K.; Voth, G. A.; Salvador, P.; Dannenberg, J. J.; Zakrzewski, V. G.; Dapprich, S.; Daniels, A. D.; Strain, M. C.; Farkas, O.; Malick, D. K.; Rabuck, A. D.; Raghavachari, K.; Foresman, J. B.; Ortiz, J. V.; Cui, Q.; Baboul, A. G.; Clifford, S.; Cioslowski, J.; Stefanov, B. B.; Liu, G.; Liashenko, A.; Piskorz, P.; Komaromi, I.; Martin, R. L.; Fox, D. J.; Keith, T.; Al-Laham, M. A.; Peng, C. Y.; Nanayakkara, A.; Challacombe, M.; Gill, P. M. W.; Johnson, B.; Chen, W.; Wong, M. W.; Gonzalez, C.; and Pople, J. A. *Gaussian03*; Gaussian, Inc.: Wallingford, CT, 2004. (b) . Gaussian 09, Revision C.01, Frisch, M. J.; Trucks, G. W.; Schlegel, H. B.; Scuseria, G. E.; Robb, M. A.; Cheeseman, J. R.; Scalmani, G.; Barone, V.; Mennucci, B.; Petersson, G. A.; Nakatsuji, H.; Caricato, M.; Li, X.; Hratchian, H. P.; Izmaylov, A. F.; Bloino, J.; Zheng, G.; Sonnenberg, J. L.; Hada, M.; Ehara, M.; Toyota, K.; Fukuda, R.; Hasegawa, J.; Ishida, M.; Nakajima, T.; Honda, Y.; Kitao, O.; Nakai, H.; Vreven, T.; Montgomery, J. A.; , Jr., Peralta, J. E.; Ogliaro, F.; Bearpark, M.; Heyd, J. J.; Brothers, E.; Kudin, K. N.; Staroverov, V. N.; Keith, T.; Kobayashi, R.; Normand, J.; Raghavachari, K.; Rendell, A.; Burant, J. C.; Iyengar, S. S.; Tomasi, J.; Cossi, M.; Rega, N.; Millam, J. M.; Klene, M.; Knox, J. E.; Cross, J. B.; Bakken, V.; Adamo, C.; Jaramillo, J.; Gomperts, R.; Stratmann, R. E.; Yazyev, O.; Austin, A. J.; Cammi, R.; Pomelli, C.; Ochterski, J. W.; Martin, R. L.; Morokuma, K.; Zakrzewski, V. G.; Voth, G. A.; Salvador, P.; Dannenberg, J. J.; Dapprich, S.; Daniels, A. D.; Farkas, O.; Foresman, J. B.; Ortiz, J. V.; Cioslowski, J.; Fox, D. J. *Gaussian09*; Gaussian, Inc.: Wallingford, CT, 2010.

(29) Torres, E.; DiLabio, G. A. *J. Phys. Chem. Lett.* **2012**, *3*, 1738−1744.

(30) Johnson, E. R.; Salamone, M.; Bietti, M.; DiLabio, G. A. *J. Phys. Chem. A* **2013**, *117*, 947−952.

(31) Boys, S. F.; Bernardi, F. *Mol. Phys.* **1970**, *19*, 553−566.

(32) Bader, R. F. W. *Atoms in Molecules: A Quantum Theory*; Clarendon Press: Oxford, U.K., 1990.

(33) Biegler-Konig, F.; Schonbohm, J.; Derdau, R.; Bayles, D.; Bader, R. F. W. *AIM 2000*, version 1; Büro für Innovative Software: Bielefeld, Germany, 2000.

(34) Glendening, E.D.; Badenhoop, J. K.; Reed, A. E.; Carpenter, J. E.; Bohmann, J. A.; Morales, C. M.; Landis, C. R.; , Weinhold, F. *NBO 6.0*; Theoretical Chemistry Institute, University of Wisconsin: Madison, WI, 2013; http://nbo6.chem.wisc.edu/.
(35) Dennington, R., II; Keith, T.; Millam, J.; Eppinnett, K.; Hovell, W. L.; Gilliland, R. *GaussView*, Version 3.09; Semichem, Inc.: Shawnee Mission, KS, 2003.
(36) Batsanov, S. S. *Inorg. Mater.* **2001**, *37*, 871−885.
(37) Koch, U.; Popelier, P. L. A. *J. Phys. Chem.* **1995**, *99*, 9747−9754.
(38) Aiswarya Lakshmi, P. Ph.D. Thesis, Indian Institute of Science, Bangalore, India, 2011.
(39) Politzer, P.; Lane, P.; Concha, M. C.; Ma, Y.; Murray, J. S. *J. Mol. Model.* **2007**, *13*, 305−311.
(40) Metrangolo, P.; Meyer, F.; Pilati, T.; Resnati, G.; Terraneo, G. *Angew. Chem., Int. Ed.* **2008**, *47*, 6114−6127.
(41) Legon, A. C. *Phys. Chem. Chem. Phys.* **2010**, *12*, 7736−7747.
(42) Karan, N. K.; Arunan, E. *J. Mol. Struct.* **2004**, *688*, 203−205.
(43) Jeffrey, G. A.; Saenger, W. *Hydrogen Bonding in Biological Structures*; Springer Verlag: Berlin, Germany, 1991.
(44) Klein, R. A. *Chem. Phys. Lett.* **2006**, *425*, 128−133.
(45) Mandal, P. K.; Arunan, E. *J. Chem. Phys.* **2001**, *114*, 3880−3882.
(46) Raghavendra, B.; Mandal, P. K.; Arunan, E. *Phys. Chem. Chem. Phys.* **2006**, *8*, 5276−5286.